



ELSEVIER

Nuclear Instruments and Methods in Physics Research B 197 (2002) 11–16

**NIM B**  
Beam Interactions  
with Materials & Atoms

www.elsevier.com/locate/nimb

# Monte Carlo simulation of kilovolt positron penetration and backscattering probabilities in solids

Asuman Aydın \*

*Faculty of Science and Literature, Department of Physics, Balıkesir University, 10100 Balıkesir, Turkey*

Received 4 February 2002; received in revised form 23 July 2002

## Abstract

Monte Carlo simulations of the backscattering probabilities, mean penetration depths and implantation profiles of positrons for elemental solids are reported as a function of atomic number  $4 \leq Z \leq 82$  and incident energies from 5 to 70 keV. It is demonstrated that backscattering probability and mean penetration depth values can be estimated reliably by using a simple Monte Carlo code for different incident energies and angles. The simulation results are in general in good agreement with other simulations and experiments.

© 2002 Elsevier Science B.V. All rights reserved.

*Keywords:* Monte Carlo; Positron; Backscattering; Implantation profile; Mean depth

## 1. Introduction

The energy loss of positrons penetrating solid matter has been a subject of interest for several years due to its applications in various surface investigation techniques. In some cases, the backscattering probability is the main feature of interest; in other cases, it has become a matter of interest to compute, for example the energy loss distributions of positrons transmitted and reflected through thin layers and backscattered semi-infinite solids by means of the Monte Carlo method. Generally, the method of Monte Carlo simulation has been used to calculate the scattering and energy loss of the charged particles penetrating

matter. The introduction of this method to the scattering of positrons up to 70 keV has stimulated the practical application of elastic and inelastic scattering differential cross-sections, and also a simple Monte Carlo code which works in a wide range of energy for many metals.

The purpose of present work was to develop further evidence of accuracy of the Monte Carlo method for positrons traversing low and high  $Z$  materials (beryllium, silicon, copper, tin and lead) with initial energies from 5 to 70 keV. In this calculations a simple modified version of a Monte Carlo code, which was previously developed by us, has been used [1,2]. The output of the Monte Carlo code consists of implantation profiles and energy spectra of backscattered positrons.

The interactions of positrons, while passing through matter, are elastic and inelastic collisions with atoms, annihilation in flight or rest, and the

\* Tel.: +90-266-249-3358; fax: +90-266-245-6366.

E-mail address: [aydina@balikesir.edu.tr](mailto:aydina@balikesir.edu.tr) (A. Aydın).

creation of bremsstrahlung radiation, where the atomic collision processes are dominant at the initial positron energies studied in the present work. Because of the latter fact, the creation of bremsstrahlung radiation and the annihilation of positrons in flight or rest are ignored.

## 2. Method

Several techniques for the simulation of elastic and inelastic interactions of electrons and positrons have been developed and adopted in Monte Carlo programs. The Monte Carlo code used here to model positron implantation is based on Monte Carlo programs developed by Valkealahti and Nieminen [3], Jensen and Walker [4], Aers [5], Ghosh and Aers [6], Fernández-Varea et al. [7] and references there in.

The Monte Carlo code developed by Fernández-Varea et al. [7] for the simulation of the transport of low energy electrons and positrons in solids, includes a critical discussion of concepts and approximations in the scattering model. In their work, inelastic scattering is calculated using a Bethe surface model based on optical and photoelectric data for the solid, making possible a good accuracy at low energies. Elastic scattering is calculated by means of a differential cross-section obtained by relativistic partial wave analysis for an exchange-corrected muffin-tin Dirac–Hartree–Slater atomic potential. The Monte Carlo simulation method of Jensen and Walker [4] is based on either the Penn dielectric loss function or the Lindhard dielectric function to model inelastic scattering and elastic scattering cross-sections obtained from a partial wave expansion for the transport of high energy (1–50 keV) positrons and electrons in solids.

Coleman et al. [8] reported on measurements and Monte Carlo simulations of the total coefficients for the backscattering of positrons as a function of atomic number  $Z$  between 13 and 82, and incident energies from 1 to 50 keV. Mäkinen et al. [9] measured the backscattering probability as a function of the incident positron energy in the range 2–30 keV and the atomic number  $Z$  of the target  $6 \leq Z \leq 79$  by using a magnetically guided positron beam.

The main physical ingredients in our code are the total elastic and inelastic cross-sections, the elastic differential cross-section, and the energy loss distribution for the inelastic scattering. Elastic scattering cross-sections were obtained from the screened Rutherford differential cross-section with a spin-relativistic factor [10] and some extra total cross-section information at low energies [11–13]. For inelastic scattering Liljequist’s model [14] were used to calculate the total inelastic scattering cross-section. The energy loss in the inelastic scattering process was sampled using Gryzinski’s excitation function [15]. Treatment of the elastic and inelastic collision contains several approximations. The total cross-sections could have uncertainties. Therefore the total cross-section values were optimized. Total cross-section expressions used in the Monte Carlo code were obtained by fitting the values calculated from various approximations [10,14,15]. The Monte Carlo program calculates the positron backscattering probabilities as a function of the incident energy in the range 5–70 keV and the target atomic number  $4 \leq Z \leq 82$  at various incident angles normal to solid surface. The positrons have been followed in a semi-infinite medium until they have backscattered or slowed down below 50 eV. A large number ( $10^4$ ) of positron trajectories were followed through the target material as they interact with the target atoms via both elastic and inelastic processes. The detailed description of the physical ingredients involved has been previously reported [2,11].

## 3. Results and conclusions

The accuracy of Monte Carlo code was tested in two ways: (a) by comparison with other Monte Carlo codes, (b) by comparison with the experimental backscattered and mean depth coefficients.

Fig. 1 shows the calculated backscattering probabilities for positrons entering normally into the semi-infinite targets as a function of energy. Inset of Fig. 1 shows the dependence of backscattering probabilities on atomic number for 5, 20 and 50 keV positron energies. The backscattering probabilities increase with increasing atomic number for Be, Si, Cu, Sn and Pb. Fig. 2(a)–(d)

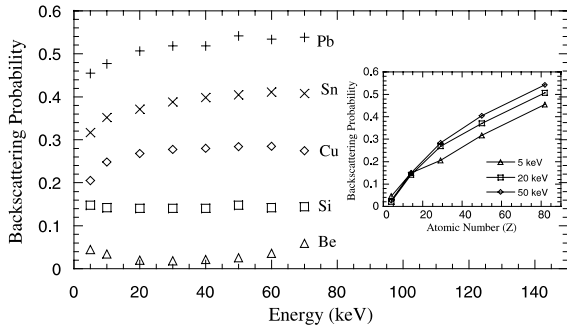


Fig. 1. Backscattering probabilities entering normally into the targets versus incident positrons energies.

represent the comparisons with other Monte Carlo results and available experimental data for the energy dependence of backscattering probabilities of positron at normal incidence. Fig. 2(a) shows the calculated backscattering probabilities for beryllium target with other Monte Carlo data given by Coleman et al. [8], Jensen and Walker [4], Fernández-Varea et al. [7]. As seen from Fig. 2(a) the backscattering probabilities of Fernández-Varea et al. [7] are smaller than the results of

Jensen and Walker [4], especially starting from the incident energy of positron 5 keV, however our results are in good agreement with the results of Fernández-Varea et al. [7] for energy range of 10–50 keV. Above 50 keV positrons energies, this agreement is missing due to different calculation methods for elastic and inelastic scattering cross-sections. Fig. 2(b) shows the calculated backscattering probabilities for silicon target with experimental and Monte Carlo results given by Mäkinen et al. [9] Fig. 2(c) shows the calculated backscattering probabilities for copper target with experimental results of Coleman et al. [8], and with other Monte Carlo data reported by Coleman et al. [8], Jensen and Walker [4], Aers [5], Ghosh and Aers [6] and, Fernández-Varea et al. [7]. Fig. 2(d) shows the calculated backscattering probabilities for lead target with the Monte Carlo data given by Berger [16]. Judging from experimental data on backscattering from gold [8], the calculated backscattering probabilities for lead are higher than what is expected at low energies. The Born approximation, which generates the screened Rutherford cross-section used in the code, exaggerates

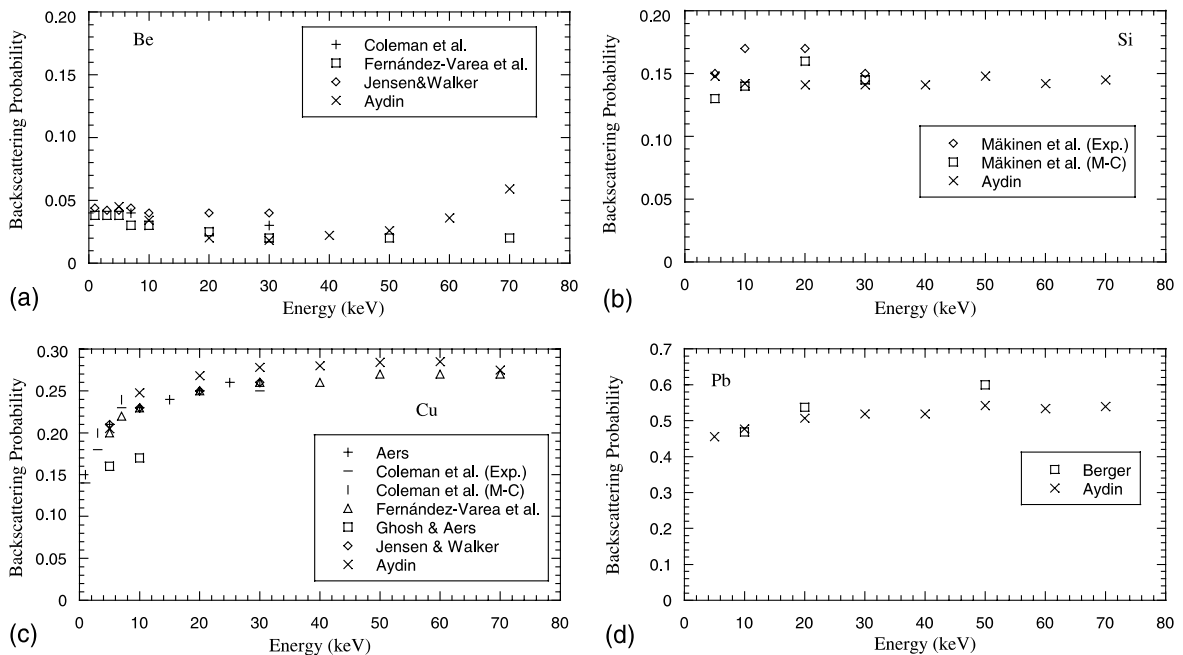


Fig. 2. Comparison of backscattering probabilities of positrons for (a) Be, (b) Si, (c) Cu and (d) Pb.

elastic scattering. The results are however in satisfactory agreement with other Monte Carlo and experimental results. As we compare the available experimental backscattering probabilities with our Monte Carlo results for silicon and copper, there are slight differences between them. This discrepancy has also been reported by Coleman et al. [8] and Mäkinen et al. [9]. Therefore accuracy of our simple Monte Carlo code is comparable with more advanced Monte Carlo codes, except in the limit of low energies and high atomic numbers.

The backscattering probabilities were calculated for positrons entering into the semi-infinite targets at various angles for positron energies from 5 to 70 keV. The backscattering probabilities increase with increasing incident angle. Fig. 3 shows the energy distribution of backscattered positrons in semi-infinite targets of 0° (a) and 75° (b) incident angles for 50 keV the positron energy.

The mean penetration depths  $\langle z \rangle$  were calculated by fitting the implantation profiles with the distribution function of Eq. (1) suggested by Valkealahti and Nieminen [3],

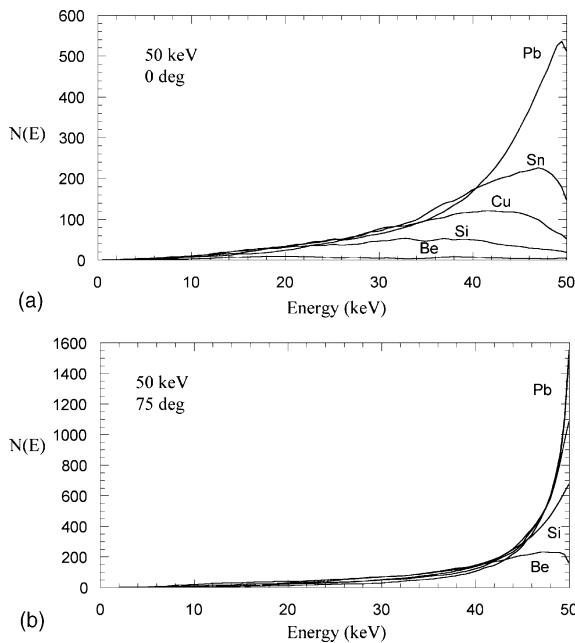


Fig. 3. Energy distributions of backscattered positrons for 50 keV positron energy at the incident angle of (a) 0° and (b) 75°.

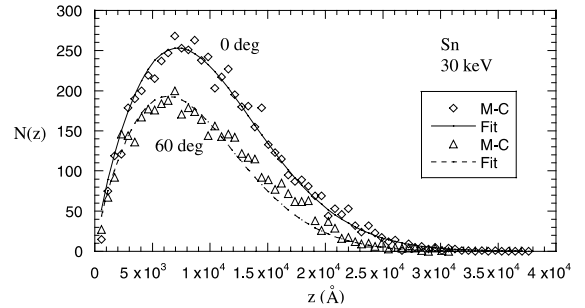


Fig. 4. Typical implantation profiles of positrons at 10 keV (at 15° and 75°) in the semi-infinite Sn.

$$P(z) = (mz^{m-1}/z_0^m) \exp[-(z/z_0)^m], \quad (1)$$

where  $z$  is the penetration depth,  $z_0$  and  $m$  are parameters to be determined by fit. Typical implantation profiles for positrons at various angles and energy are shown in Fig. 4.

Fig. 5 presents the calculated mean penetration depth  $\langle z \rangle$  of positrons as a function of their energy at normal angle. Inset of Fig. 5 shows the dependence of mean penetration depth  $\langle z \rangle$  of positrons as a function of their energy at 45° the incident angle. As can be seen in Fig. 5, the mean penetration depth values are slightly smaller at the incident angle of 45°. Fig. 6 shows the comparison of mean penetration depths with the results of Jensen and Walker [4] for beryllium and with those of Aers [5], Ghosh and Aers [6], Jensen and Walker [4] and Valkealahti and Nieminen [3] for copper. Our results are in satisfactory agreement with other Monte Carlo results. Fig. 7 shows the energy

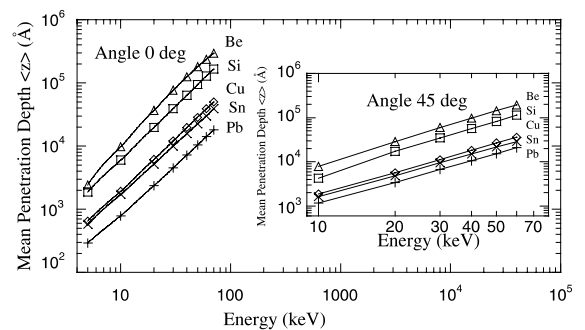


Fig. 5. Mean penetration depths  $\langle z \rangle$  entering 0° and 45° into the targets as a function of positrons energies.

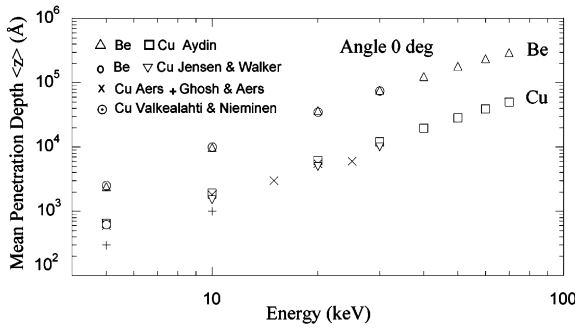
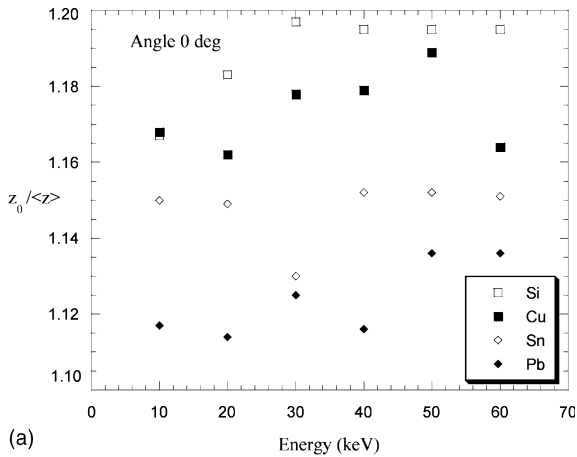
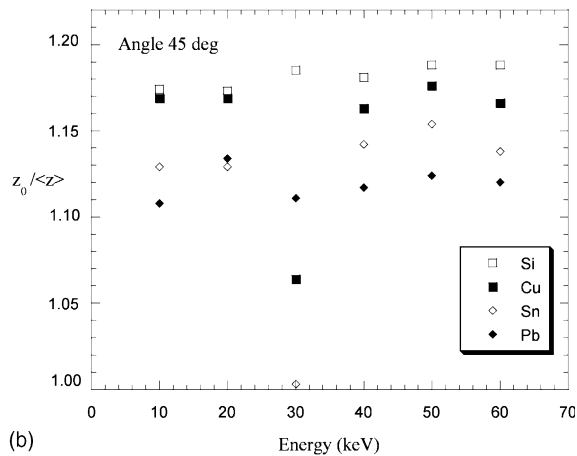


Fig. 6. Comparison of mean penetration depths  $\langle z \rangle$  entering normally into the Be and Cu targets as a function of positrons energies.



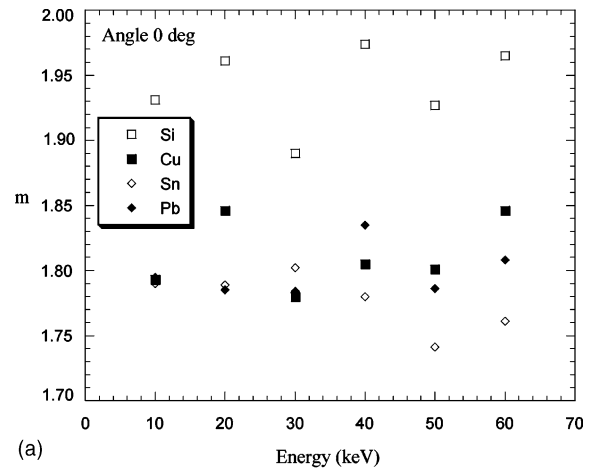
(a)



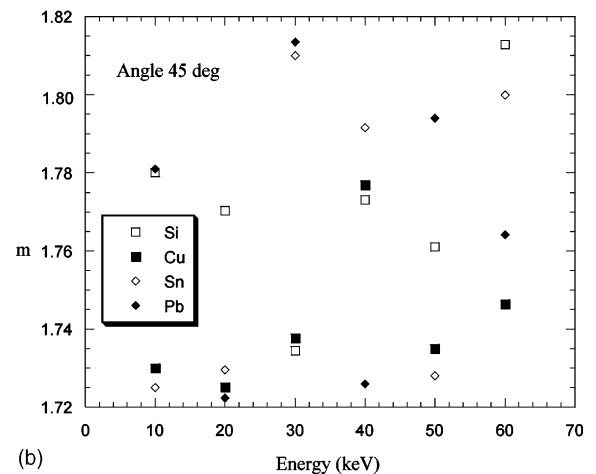
(b)

Fig. 7. Ratio  $z_0 / \langle z \rangle$  versus energy at the incident angle of (a)  $0^\circ$  and (b)  $45^\circ$ .

dependence of the ratio  $z_0 / \langle z \rangle$  in semi-infinite targets with  $0^\circ$  (a) and  $45^\circ$  (b) incident angles. Fig. 8 also presents the energy dependence of the parameter  $m$  at the same angles. This approach could be extended to cover other incident angles, and the  $z_0 / \langle z \rangle$  ratio and  $m$  parameter have been found close to each other. The calculated  $z_0 / \langle z \rangle$  ratio has a weak energy dependence with the values of 1.17 at 10 keV and 1.20 at 60 keV for silicon and of 1.12 or 1.14 for lead at the same energies and normal angle. The average value of  $z_0 / \langle z \rangle$  is 1.19 for silicon, 1.17 for copper, 1.15 for tin and 1.12 for lead at normal angle. The parameter  $m$  in Eq. (1) also has a small energy dependence; it is equal to 1.93 at 10 keV and 1.97 at 60 keV for silicon, and 1.80



(a)



(b)

Fig. 8. Parameter  $m$  of Eq. (1) as a function of energy at the incident angle of (a)  $0^\circ$  and (b)  $45^\circ$ .

or 1.81 for lead at the same energies and normal angle. The average value of  $m$  is 1.94 for silicon, 1.81 for copper, 1.78 for tin and 1.80 for lead.

In summary, the backscattering probabilities of positrons and the mean penetration depths were calculated for various semi-infinite solid targets in the energy ranges 5–70 keV. The results are mostly in good agreement with the others reported in the literature. The experimental backscattering coefficients are compatible with the present understanding of elastic and inelastic scattering processes and the simple description of positron transport implied by the present Monte Carlo method.

## References

- [1] A. Aydın, Rad. Phys. Chem. 59 (2000) 277.
- [2] A. Aydın, Nukleonika 46 (3) (2001) 87.
- [3] S. Valkealahti, R.M. Nieminen, Appl. Phys. A 32 (1983) 95.
- [4] K.O. Jensen, A.B. Walker, Surf. Sci. 292 (1993) 83.
- [5] G.C. Aers, J. Appl. Phys. 76 (3) (1994) 1622.
- [6] V.J. Ghosh, G.C. Aers, Phys. Rev. B 51 (1) (1995) 45.
- [7] J.M. Fernández-Varea, D. Liljequist, S. Csillag, R. Rätty, F. Salvat, Nucl. Instr. and Meth. B 108 (1996) 35.
- [8] P.G. Coleman, L. Albrecht, K.O. Jensen, A.B. Walker, J. Phys. Condens. Mat. 4 (1992) 10311.
- [9] J. Mäkinen, S. Palko, J. Martikainen, P. Hautojärvi, J. Phys. Condens. Mat. 4 (1992) L503.
- [10] S.M. Seltzer, Appl. Radiat. Isot. 42 (1991) 917.
- [11] E.N. Özmütlu, A. Aydın, Appl. Radiat. Isot. 45 (9) (1994) 963.
- [12] E.N. Özmütlu, A. Aydın, Appl. Radiat. Isot. 47 (2) (1996) 185.
- [13] E.N. Özmütlu, A. Aydın, Appl. Radiat. Isot. 48 (3) (1997) 403.
- [14] D. Liljequist, J. Phys. D: Appl. Phys. 16 (1983) 1567.
- [15] M. Gryzinski, Phys. Rev. A 138 (1965) 305, 322, 336.
- [16] M.J. Berger, App. Radiat. Isot. 42 (10) (1991) 905.